Supplementary Materials for

Serial interval of SARS-CoV-2 was shortened over time by nonpharmaceutical interventions

Sheikh Taslim Ali*, Lin Wang*, Eric H. Y. Lau*, Xiao-Ke Xu, Zhanwei Du, Ye Wu, Gabriel M. Leung, Benjamin J. Cowling†

*These authors contributed equally to this work.
†Corresponding author. Email: bcowling@hku.hk

Published 21 July 2020 on *Science* First Release
DOI: 10.1126/science.abc9004

This PDF file includes:

Other Supplementary Material for this manuscript includes the following:
(available at science.sciencemag.org/cgi/content/full/science.abc9004/DC1)

MDAR Reproducibility Checklist (.pdf)

Table of Contents

Materials and Methods

1. Reconstruction of transmission pairs

In mainland China, 27 provincial and 264 urban health commissions publicly posted detailed reports (in Chinese) of 9,120 confirmed COVID-19 cases online during January 15 – February 29, 2020, which comprised 72.7% of all COVID-19 cases confirmed in mainland China outside Hubei Province. The original reports were the results of contact tracing and epidemiological investigations conducted by health authorities in mainland China. Each of the original case reports provides a detailed description on the demographic information (e.g., age, sex, job, residential city), travel history (e.g., returned from Hubei, transferred at Wuhan, never travelled recently), potential contacts (e.g., close contacts, face-to-face proximity), social relationships with the contacts (e.g., familial member, classmate, colleague), and epidemiological timelines if known (e.g., potential times of infection, symptom onset, hospital visit(s), isolation, confirmation, and public disclosure). By screening all of these reported cases independently by three co-authors, we reconstructed 1,407 transmission pairs using the following protocols (*31*): (1) We first identified a pair or a group of confirmed cases by the information on their close contacts or familial ties. Specifically, we used the following criteria to determine whether two cases had a transmission pair due to the existence of close contact: (i) A clear statement of the keyword "close contacts" (密切接触 in Chinese); (ii) Statements indicating the existence of face-to-face proximity or physical contacts, such as "shared a meal (聚餐 in Chinese)", "travelled together (自驾与亲属某某同行 in Chinese)", "worked together (一起进行工作 in Chinese)".(2) For an identified transmission pair reported with familial relationship between two cases, we used this familial relationship to determine whether it was household or non-household transmission. Specifically, we used the immediate familial relationships (e.g., a person's spouse,

parents, and children) as the indicator of household transmission, and all other familial relationships (e.g., a person's siblings with age ≥17) as well as close contacts without familial information as the indicator of non-household transmission.

(3) We then determined the infector and infectee of each transmission pair according to their travel histories and locations of exposure. When two cases were reported with a single epidemiological link (i.e., no other case involved in their transmission), they often had a straightforward transmission direction as follows: The infector had a recent travel history linked to Hubei province or a close contact with other case(s) recently visited Hubei province, whereas although reported with no recent travel history to Hubei province, the infectee had a close contact with the infector and no close contacts with people returned from other provinces. When a case had several possible infectors after evaluating their travel histories and exposure locations, we assumed that the infector of this transmission pair was the one who first developed symptom. Such situation was observed for some household transmissions. For example, given three confirmed cases *i*, *j*, and *k* from the same household outside Hubei province and only two family members *i* and *j* recently visited Hubei, case *k* could be infected by either case *i* or *j*, which is difficult to infer if the exposure times of cases *i* and *j* were not available from their public reports. As a simplification, we chose the infector of case *j* as the family member (*i* or *j*) with the earliest symptom onset. Our recent study (*31*) has validated the robustness of this approximation.

2. Stratifications of transmission pairs

Along with the stratification by household settings(as defined in protocol 2 in above section), we also stratified transmission pairs by the isolation delay, age, or sex.. Denote the *isolation delay* as the time duration from the symptom onset to isolation time for the infector of each transmission

pair. The s*horter* (*longer*) *isolation delay* is used to find the transmission pairs with isolation delays shorter (longer) than the median isolation delay across those transmission pairs that are identified by a given stratification condition (e.g., household transmission). The *younger-age* (*older-age*) are used to find the transmission pairs with infectors younger (older) than the median age across all infectors of those transmission pairs that are identified with a given condition (e.g., household transmission). The indicator *male* and *female* are defined similarly.

3. Estimation of serial interval distribution

Given a reconstructed transmission pair, the serial interval was computed as the number of days between the reported symptom onset date of the infector and of the infectee. Serial interval distribution was estimated by fitting a normal (or Gumbel) distribution to the corresponding data via Markov Chain Monte Carlo (MCMC) with Gibbs sampling and non-informative flat prior. Normal distribution is a representative of symmetric distribution, and Gumbel distribution is a representative of asymmetric distribution. To fit a normal distribution, we estimated the mean and standard deviation of the normal distribution; to fit a Gumbel distribution, we estimated the location and scale parameters of the Gumbel distribution. We confirmed the convergence of MCMC chains via trace plot and diagnosis. We obtained the posterior distribution of parameters by running 100,000 iterations with a burn-in of 40,000 iterations and a thinning interval of 10.

4. Mechanisms underlying the observed patterns

From the view of a single transmission pair, the serial interval depends on the infectiousness profile of the infector and the incubation period of the infectee. On the other hand, from the view of each infector, the realized serial intervals may not only depend on the properties of each

transmission pair (i.e., infectiousness profile, incubation period) but may also depend on the properties of contacts (e.g., contact patterns (*22, 32*), structure of contacts (*33, 34*). Fig. S1 (A) illustrates the effect of these basic factors on shaping serial interval distribution.

The influence of non-pharmaceutical intervals (NPIs) on re-shaping serial interval distribution can be understood from two aspects (Fig. S1 (B)-(C)). On one hand, the implementation of NPIs via enhanced contact tracing and scaling up testing capacities reduced the time delay in isolating cases (Fig. S2), which reduces the period of infectiousness and hence truncates the exposure window for susceptible individuals to acquire infection. On the other hand, the NPI-induced truncation on the period of infectiousness may also reduce or even avoid the generation of some secondary cases, skewing the serial interval distribution to the left.

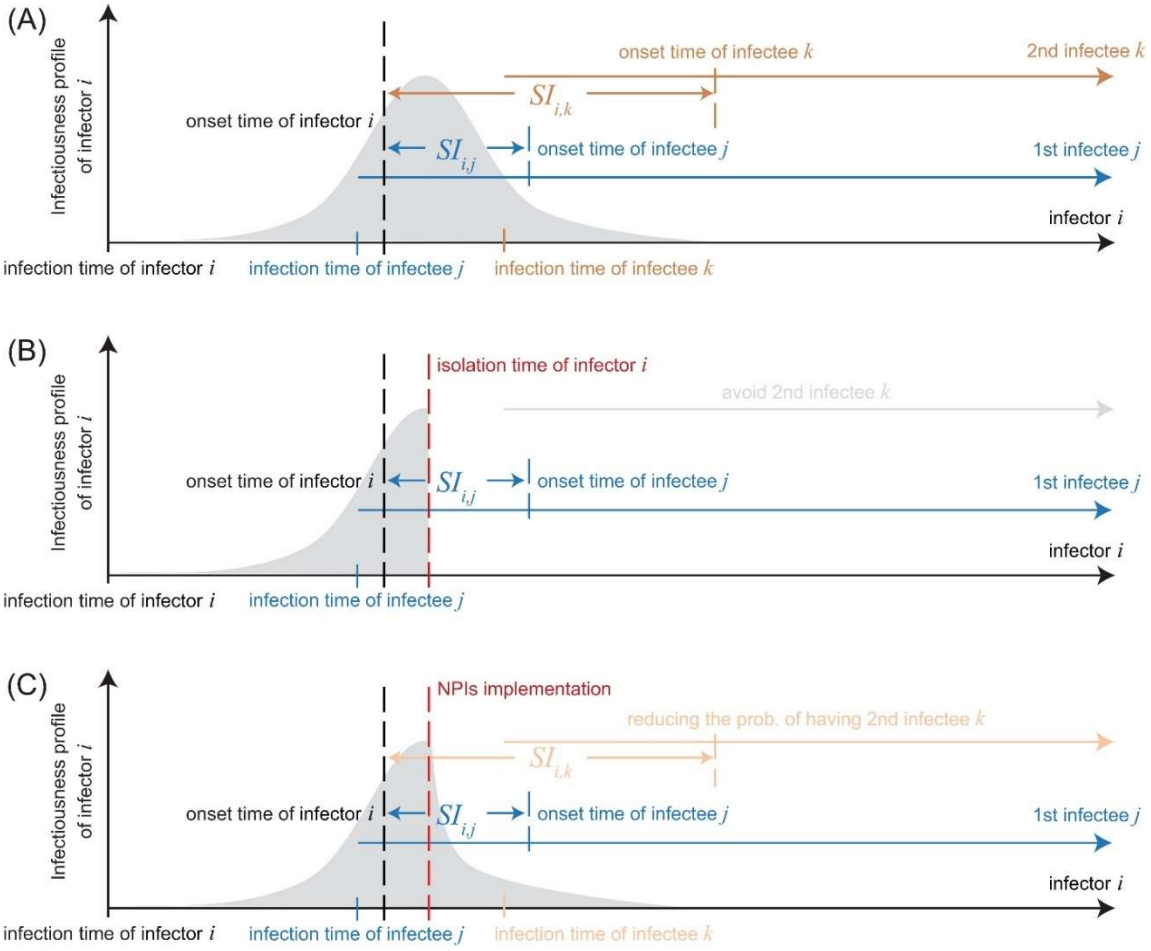

Fig. S1: Illustration for the influence of non-pharmaceutical intervals (NPIs) on changing serial interval distribution. (A) Without NPIs, the distribution of serial intervals depends on the properties of contacts (e.g., contact patterns, structure of contacts) and properties of transmission pair (e.g., infectiousness profile, incubation period). (B) Rapid case identification and isolation can abruptly truncate the infectiousness profile of an infector, avoiding the generation of some secondary cases thereon. (C) Other NPIs (e.g., lockdown, confinement, travel restrictions) may reduce overall infectiousness but some were triggered by symptoms and hence have a larger effect on infectiousness after symptom onset. The overall effect narrows the infectiousness profile of an infector, lowering the probability in generating secondary cases.

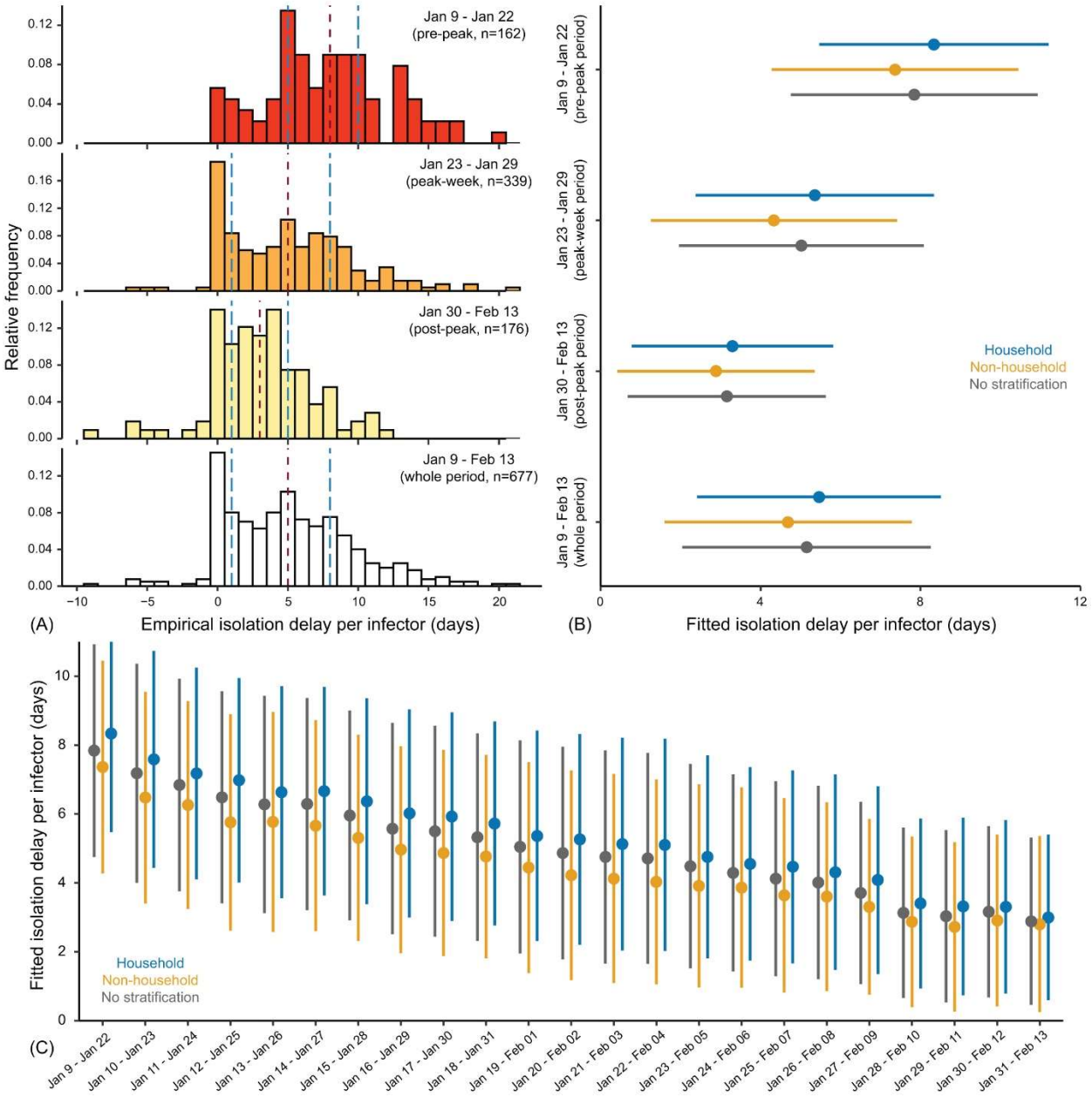

Fig. S2: Temporal change of the time delay in isolating COVID-19 infectors from their symptom onset (i.e., isolation delay) in mainland China. (A) Empirical isolation delay distributions. From top to bottom, transmission pairs were analyzed by selecting infectors who developed symptoms during January 9 − 22, 2020 (pre-peak), January 23 − 29, 2020 (peak-week), January 30 − February 13, 2020 (post-peak), and January 9 − February 13, 2020 (whole period), respectively. In each panel, vertical dashed lines in red and blue colors indicate the median and interquartile range (IQR). (B) Estimated isolation delay distributions by fitting a normal distribution to isolation delay data via MCMC. From top to bottom, each group of bars correspond to the transmission pairs with infectors who developed symptom during the pre-peak, peak-week, post-

peak, and whole 36-day period, respectively. Colored dots and bars correspond to the transmission pairs within households (blue), outside households (yellow), and transmission pairs with no stratification (dark-grey). (C) Estimated isolation delay distribution for each running time window by fitting a normal distribution. Dark-grey color indicates fitting data with no stratification, whereas blue (yellow) indicates fitting household (non-household) data. Dots and bars in (B) and (C) indicate the estimated median and IQR, respectively.

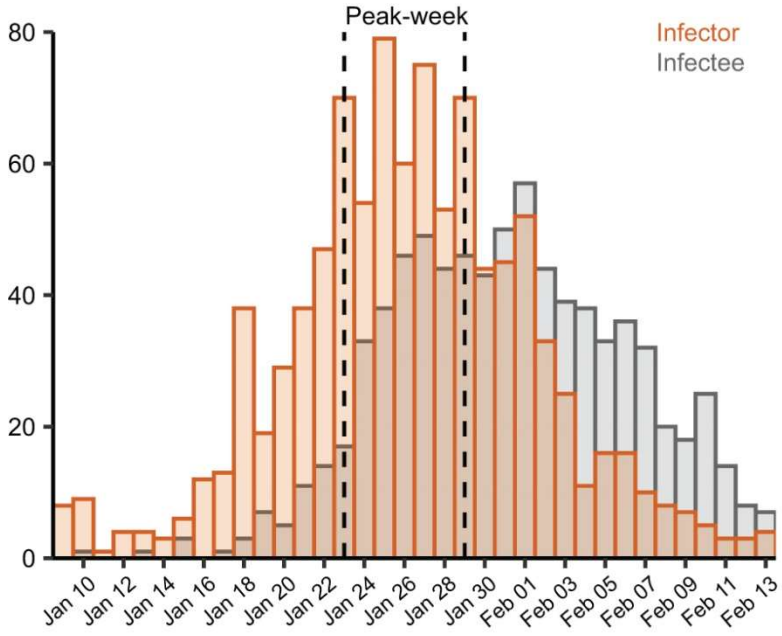

Fig. S3: Daily number of COVID-19 infectors (orange bar) and infectees (grey bar) by their symptom onset in China outside Hubei province during January 9 – February 13, 2020. The 1-week period during January 23 – 29, 2020, is regarded as the peak-week period, because a large number of infectors (339, ~50% of data) developed symptom during this week. The earlier14-day period (January 9–22, 2020) is regarded as the pre-peak period, and the later 15-day period (January 30 – February 13, 2020) is regarded as the post-peak period.

5. Effect of non-pharmaceutical interventions on shortening effective serial intervals over time

This section tests the hypotheses (illustrated in the above section and Fig. S1) for the effect of NPIs on shortening serial intervals over time, by using a probabilistic model (section 5.1), individual-based simulations (section 5.2) and regression models (section 5.3)

5.1 Probabilistic model of transmission pair

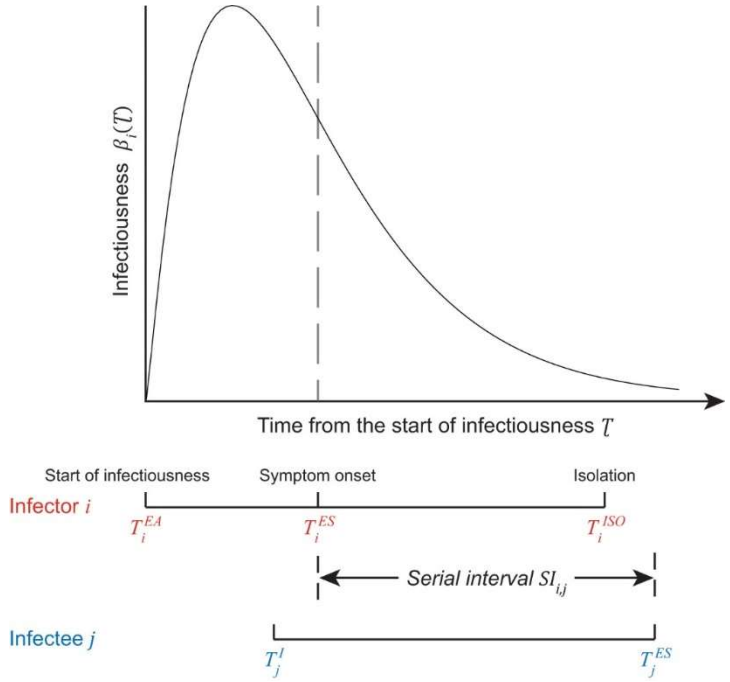

Fig. S4. Schematic of a transmission pair. The infector i starts to be infectious and symptomatic, and then is isolated at time T_i^{EA}, T_i^{ES}, and T_i^{ISO}, respectively. The infectee j is infected by the infector i at time T_j^I and becomes symptomatic at time T_j^{ES}. Top panel illustrates the infectiousness profile of infector i, which is assumed to follow a gamma distribution.

Given a transmission pair in which the infectee j is infected by the infector i at time T_j^I, the serial interval denotes the time duration between the symptom onset time of infector T_i^{ES} and symptom onset time of infectee T_j^{ES}: $SI_{i,j} = T_j^{ES} - T_i^{ES}$.

Denote T_i^{EA} as the time at which the infector *i* starts to be infectious, T_i^{ISO} the time at which the infector *i* is isolated, and $D_i = T_i^{ISO} - T_i^{ES}$ the time delay from symptom onset to isolation of infector *i*, respectively. We term D_i as the isolation delay.

Following He et al. (*20*), we define the infectiousness of infector *i* as the probability to infect an infectee $\tau = T_j^I - T_i^{EA}$ days after infector *i* starts to be infectious at time T_i^{EA}. The probability density function (pdf) of infectiousness is assumed to follow a gamma distribution (*20*): $\beta_i(\tau) = \frac{1}{\Gamma(k)\cdot\theta^k} \cdot \tau^{k-1} \cdot \exp\left(-\frac{\tau}{\theta}\right)$, where k and θ are the shape and scale parameters, respectively. Recent clinical (*35-37*), epidemiologic (*16, 20, 38-40*), and biological studies (*41-43*) suggest that the SARS-CoV-2 infection is able to shed virus particles before symptom onset, which can cause a substantial proportion of pre-symptom transmissions. Hence we consider that the infectiousness starts from C_i days before symptom onset of infector *i*, i.e., $C_i = T_i^{ES} - T_i^{EA}$. Based on these settings, the expression of serial interval becomes:

$$SI_{i,j} = E_j^S + \tau - C_i$$

where the first term $E_j^S = T_j^{ES} - T_j^I$ is the incubation period of infectee *j*. Based on the detailed exposure history for the first 425 confirmed SARS-CoV-2 cases in Wuhan, Li et al. (*17*) suggested that the pdf of incubation period $P(E^S)$ follows a log-normal distribution with a mean of 5.22 days and standard deviation of 3.87 days.

Given an isolation delay D_i that is assumed to occur before symptom onset of infectee, the pdf of serial intervals is obtained by integrating over the range of time interval τ:

$$P(SI_{i,j}) = \int_0^{C_i+D_i} \beta_i(\tau) \cdot P(E^s = SI_{i,j} + C_i - \tau)\, d\tau$$

The cumulative distribution is given by $\int_{-\infty}^{x} P(SI_{i,j})\, dSI_{i,j}$, and the mean serial interval is given by: $\int_{-\infty}^{\infty} SI_{i,j}\, P(SI_{i,j}) dSI_{i,j}$.

To compare with data of transmission pairs in which serial interval and isolation delay were available, we also computed the pdf of serial intervals with minimum isolation delay D_i^{min}:

$$P(SI_{i,j}, D_i^{min}) = \int_{D_i^{min}}^{\infty} P(D_i) \int_0^{C_i+D_i} \beta_i(\tau) \cdot P(E^s = SI_{i,j} + C_i - \tau)\, d\tau\, dD_i$$

where $P(D_i)$ is the distribution of isolation delay D_i, which can be obtained by fitting isolation delay data.

We parameterized the start time of infectiousness C_i, and the shape k and scale θ of the gamma distribution of infectiousness with inferred results by He, X. et al. (*20*). We tested the following three scenarios which were selected from the high likelihood region estimated by He, X. et al. (*20*).

Parameters	Scenario-I	Scenario-II	Scenario-III
C_i	2 days	4 days	6 days
Shape k	2.15	2.74	1.53
Scale θ	1.34	1.71	4.38

This simple model suggests that serial intervals become shorter the faster the infectors are isolated, regardless of when an infector starts to be infectious before illness onset (fig S5).

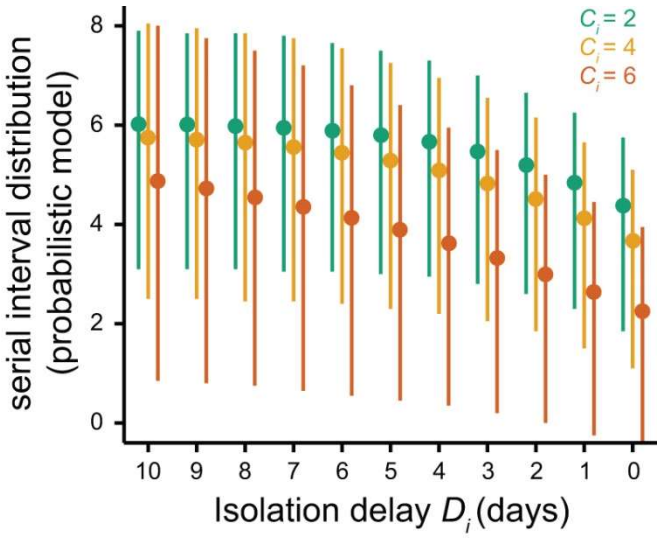

Fig. S5. Using probabilistic model to examine the effect of non-pharmaceutical interventions (NPIs) on shortening serial intervals over time. Serial intervals are estimated with the probabilistic model based on a transmission pair, in which the start time of infectiousness C_i is considered as 2 (green), 4 (yellow), or 6 (orange) days before symptom onset of infector. Given each isolation delay D_i, the dot and vertical bar indicate the mean and interquartile range (IQR) of estimated distribution.

5.2 Individual-based model for simulating serial intervals

We also simulated the serial intervals by using an individual-based model. Specifically, we started with a number of cases who have been infected at the time origin. Each potential infector will infect a number of infectees, which follows a Poisson distribution with mean R_e, the effective reproduction number. The exact infection times will be simulated according to the generation time. However, knowledge on the generation time for COVID-19 is still limited, and hence was approximated by published serial intervals, with a gamma distribution and a mean of 5.1 days (*27*), which is the same as our estimates during the peak-week period for COVID-19 in mainland China. In other scenarios, we assumed shorter and longer serial intervals respectively, which were the same as that estimated with means of 7.8 (as estimated from the pre-peak

period), 2.6 (as estimated from the post-peak period) and 8.4 days (as estimated for the 2003 SARS epidemic (*44*)). From the simulated infection times, we added the simulated incubation period for all infectees, assuming a lognormal distribution with mean 5.2 days (*17*). The duration between the symptom onset times of the infector and infectee in each transmission pair would be the simulated serial intervals. We present the mean serial intervals and their 95% confidence intervals from 500 transmission pairs in 200 simulations under different initial effective reproduction number R_e (e.g. 3.0, 2.5, 2.0, 1.5, 1.0, 0.5, 0.3) (*25*) to represent situations with different level of general control measures (e.g. social distancing, enhanced personal hygiene) in place, and reducing time delay from symptom onset to isolation (e.g. from 10 to 0 days) which was assumed to interrupt further transmission after a case has been isolated.

The results from individual-based simulations suggest the possible association between serial interval and isolation delay (Fig. S6, Table S4). Given a mean generation time of 7.8 days (as per our estimate for the pre-peak period of COVID-19 in mainland China), the simulated mean serial intervals reduces from ~8.0 to ~1.2 days when the isolation delay reduces from 10 to 0 days. Given a mean generation time of 5.1 days (as per our estimate for the peak-week period of COVID-19 in mainland China, which is similar to the estimates by Zhang *et. al.* (*27*)), the simulated mean serial interval reduces from ~5.1 to ~1.5 days when the isolation delay reduces from 10 to 0 days. Similar outcomes were obtained with alternative generation times with a mean of 2.6 days (estimate for the post-peak period) and 8.4 days (as estimated for the 2003 SARS epidemic (*44*)) (Table S4). The temporal change of serial intervals is less sensitive to the variation in initial effective reproduction number, R_e (a measure of initial transmission

accounting for the effect of control measures). Our analytical and simulated models validate that serial interval is positively associated with isolation delay.

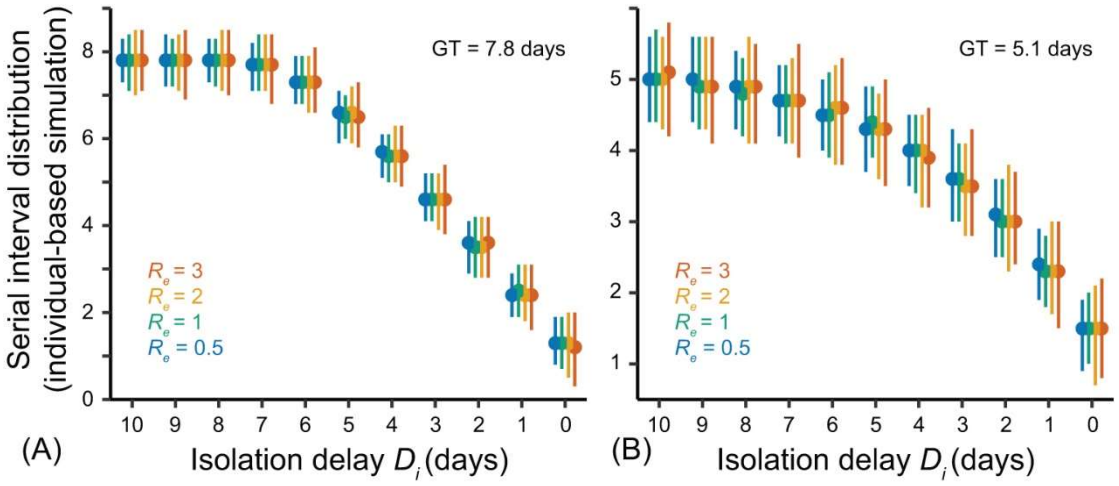

Fig. S6. Using individual-based simulation model to examine the effect of non-pharmaceutical interventions (NPI) on shortening serial intervals over time. Given each combination of isolation delay D_i and initial effective reproduction number R_e, the dots and vertical bars indicate the median and IQR of estimated distribution, when the mean generation time (GT) is 7.8 days in (A) and 5.1 days in (B).

5.3 Multivariable regression model

Since the implementation of a cordon sanitaire around Wuhan on January 23, 2020, multiple NPI strategies have been implemented in more than 260 Chinese cities, including the isolation of confirmed and suspected cases, suspension of intra-city public transport, suspension of travel between cities, social distancing by closure of entertainment and public gathering venues (e.g., bars, cinemas and parks), as well as public services (e.g., shopping malls and restaurants), and recruitment of governmental staff and volunteers to enforce quarantine (Fig. S7). To study the influence of these factors on COVID-19 transmission, we developed a series of linear univariate

and multivariable regression models to predict empirical serial intervals with infectors that developed symptoms on each day.

We evaluated the daily time series of following measures from transmission pairs. Denote, $\omega(t)$ and $d(t)$ as the observed serial interval and isolation delay on day t, respectively. We calculated $\omega(t)$ by the median of all serial intervals with infectors developed symptoms on day t, and $d(t)$ by the median of time delay from symptom onset to isolation for infectors with symptoms during day t, who caused infectees further. To quantify the daily intensity of each NPI strategy in mainland China, we also counted the number of cities in mainland China that implemented each NPI measure on day t, using the interventions data from more than 260 Chinese cities (*24*) (Fig. S7). The NPI measures include the isolation of suspected and confirmed cases, travel ban for intra-city and inter-city movement, social distancing by closing public services (e.g., hospitals, shopping malls, restaurants) and entertainment venues (e.g., cinema, bar, café) and recruiting government workers and volunteers to assist quarantine and social distancing. Denote $\eta_k(t)$ as the cumulative number of cities in mainland China that implemented the k-th intervention ($k = 1, 2, \dots, 7$) on day t..

We first used univariate linear regression models to test the association between each intervention measure and daily serial interval $\omega(t)$, and then significant factors are included one in addition to linear multi-variable regression model to predict the daily serial interval $\omega(t)$:

$$\omega(t) \sim \beta_0 d(t) + \beta_k \eta_k(t), k = 1, 2, \dots, 7$$

where each β_i is a regression coefficient for respective factors. Because the isolation delay is expected to be a prime driver of serial intervals, we considered a baseline model as $\omega_{base}(t) =$

$\beta_0 d(t)$, where $d(t)$ is the daily isolation delay (the median daily isolation delay). $\eta_1(t)$ and $\eta_2(t)$ are the daily cumulative number of cities implemented the isolation on suspected and confirmed cases respectively. The travel restrictions consist of $\eta_3(t)$ and $\eta_4(t)$, the daily cumulative number of cities implemented the inter-city and intra-city travel ban respectively. The social distancing measures are $\eta_5(t)$, $\eta_6(t)$ and $\eta_7(t)$, the daily cumulative number of cities implemented the closure of public services, closure of entertainment venues, and recruitment of government workers and volunteers to assist quarantine, respectively. Finally, we estimated the contribution of each factor according to the improvement in predicting the daily serial interval $\omega(t)$ by including each factor into the baseline model.

The univariate regression model suggests that the isolation delay is the better predictor of daily serial interval (Fig. S8). The basic regression model that only accounting for isolation delay can explain up to 51.5% of the variability in daily empirical serial interval, indicating isolation delay as the prime factor. The improved models that combine the basic model with one of either the additional factors (NPI strategy or accumulation of population immunity) can explain a further maximum of 15.6% - 16.7% variability in daily empirical serial intervals (Table S5). The model fitting further suggests a potential explanation about for how serial intervals can be modulated by respective interventions over the span of outbreak (Fig. 9). We found that, per day of early isolation, the predicted serial interval decreased by 0.7 (95% confidence interval, CI: 0.4, 0.9) days on average. Although the effects of these additional factors in combination of isolation delay are identified specifically in non-household setting, we were not able to detect their individual contribution to change serial intervals (Table S5).

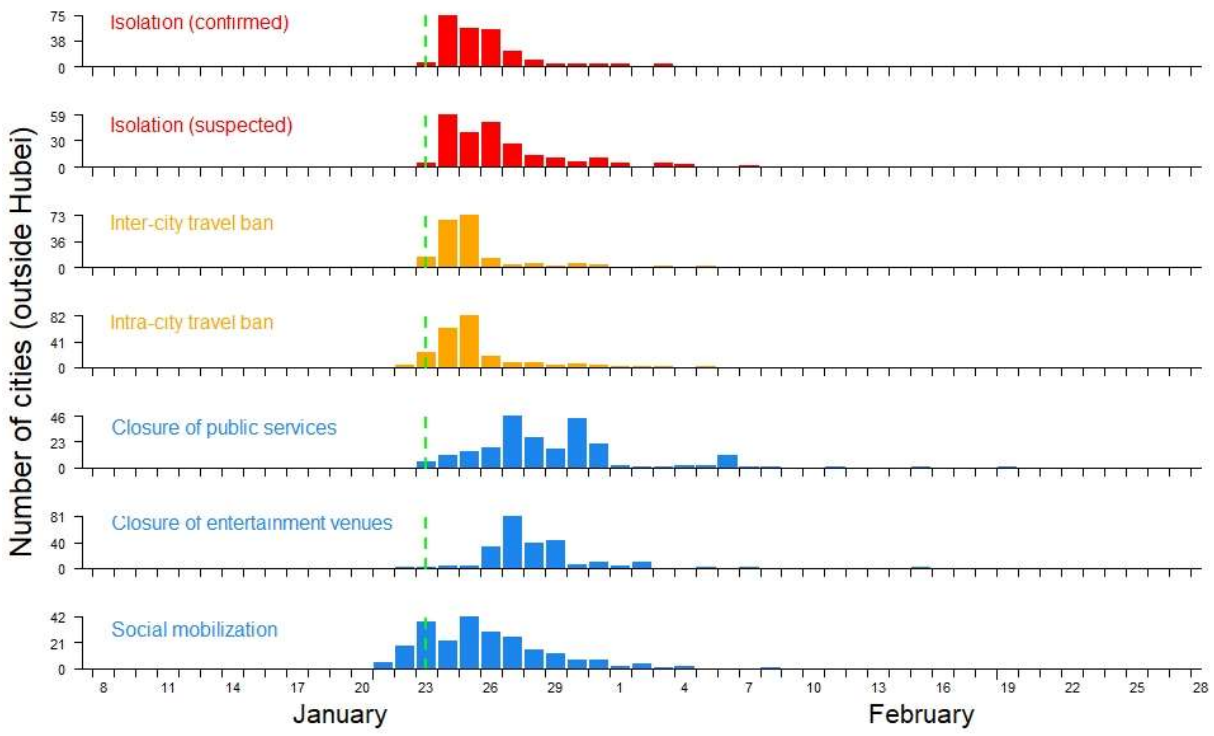

Fig. S7: Timelines for the number of Chinese cities (excluding cities in Hubei province) that were starting to implement each of the following 7 non-pharmaceutical interventions: isolation of confirmed cases, insolation of suspected cases, suspension of travel between cities (i.e., inter-city travel ban), suspension of intra-city public transport (intra-city travel ban), closure of public services (e.g., shopping malls, restaurants), closure of entertainment and public gathering venues (e.g., bar, cinema, park), and recruitment of governmental staff and volunteers to enforce quarantine (i.e., social mobilization).

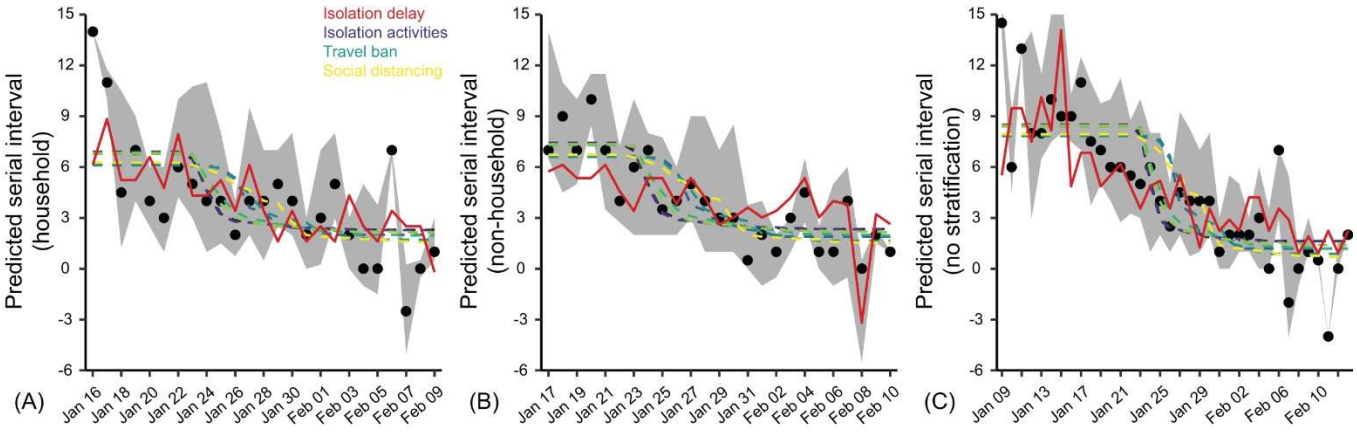

Fig. S8. The univariate regression models to examine the effect of non-pharmaceutical interventions (NPI) on shortening serial intervals over time. Prediction of empirical serial intervals with infectors that developed symptom on each day (by univariate regression models), for (A) household, (B) non-household, and (C) all transmission pairs. Black dots and grey shaded regions indicate the median and IQR of empirical serial intervals. Red curves indicate the mean of serial intervals predicted by isolation delay of infectors. Dashed curves in other colors indicate the mean serial intervals predicted by individual factors including isolating confirmed cases, isolating suspected cases, inter-city travel ban, intra-city travel ban, closure of public services, closure of entertainment venues and social mobilization.

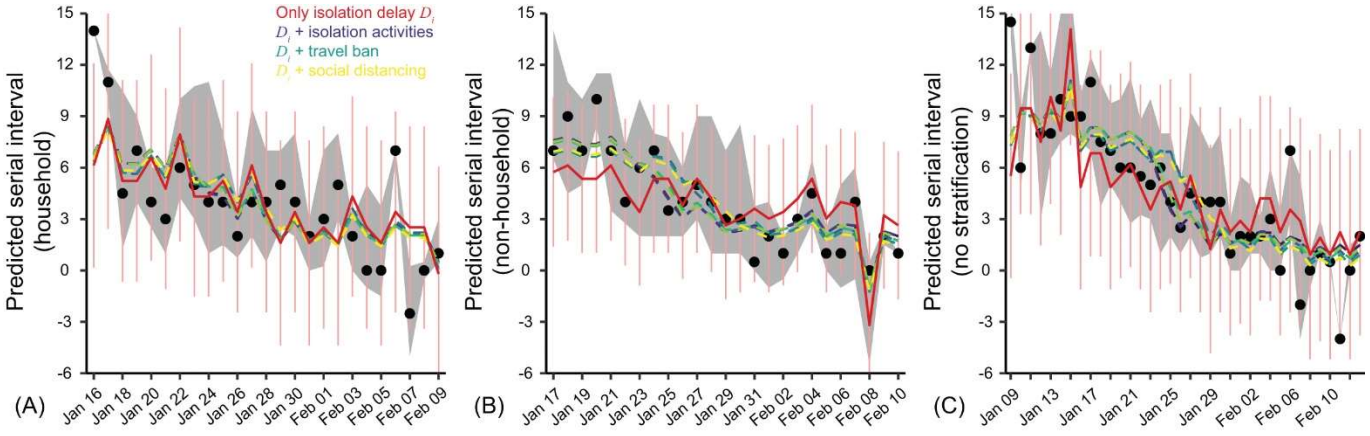

Fig. S9. The multi-variable regression models to examine the effect of non-pharmaceutical interventions (NPI) on shortening serial intervals over time. Prediction of empirical serial intervals with infectors that developed symptom on each day (by multivariable regression models), for (A) household, (B) non-household, and (C) all transmission pairs. Black dots and grey shaded regions indicate the median and IQR of empirical serial intervals. Red curves indicate the mean (with 95% confidence interval in light-pink vertical bars) of serial intervals predicted with the basic regression model only accounting for the isolation delay of infectors. Dashed curves in other colors indicate the mean serial intervals predicted by extending the basic regression model to further account for any one of the following factors: isolating confirmed cases, isolating suspected cases, inter-city travel ban, intra-city travel ban, closure of public services, closure of entertainment venues and social mobilization.

6. Real-time transmissibility estimated under a single stable serial interval distribution versus effective serial interval distributions

The real-time transmissibility of an infectious disease is often characterized by the instantaneous reproduction number (R_t), which is defined as the expected number of secondary infections caused by an infector on day t (*28, 45, 46*). The pathogen spreads when $R_t > 1$ and is under control when $R_t < 1$. To estimate R_t, a routine protocol is to approximate the generation time distribution with a single stable serial interval distribution. Let w_i be the serial interval distribution that approximates the infectiousness profile of an infected individual at i-th day since infection. Then, the daily estimate of $R_t = \frac{I_t}{\sum_{i=1}^{t} I_{t-i} w_i}$ is calculated as the ratio between the number of cases I_t on day t and the weighted average of infectiousness caused by cases infected before day t, i.e., $\sum_{i=1}^{t} I_{t-i} w_i$ (*47*).

Because we considered time-varying serial interval distributions, R_t is reconstructed as $R_t = \frac{I_t}{\sum_{i=1}^{t} I_{t-i} w_i(t)}$, in which the infectiousness $w_i(t)$ describes the probability at which individuals who are infected for i days before day *t* generate secondary infections at time t. We estimated the time-varying serial interval distribution using running time windows (Fig 2A).We compared daily R_t estimated with time-varying effective serial interval distributions versus with a single fixed serial interval distribution (Figs. 2B-D).

7. Sensitivity analyses for results validation

To validate our results, we performed following sensitivity analyses.

7.1. Sensitivity analysis on the length of running time windows and the probability distribution for fitting In the main text, we have used 14-day running time windows to estimate the real-time serial interval distributions. Here, we examined the effect of using shorter or longer length of running time windows. Using 7-day (Fig. S10A), 10-day (Fig. S10B), or 18-day (Fig. S10D) running time windows, we observed similar patterns of serial intervals shortened over time.

We also examined the alternative estimates of serial interval distributions by fitting a Gumbel distribution to data (Fig. S11). The Gumbel distribution is chosen as a representative of asymmetric distributions. Using other asymmetric distributions (e.g., Logistic distribution (*31*)) should give similar conclusions.

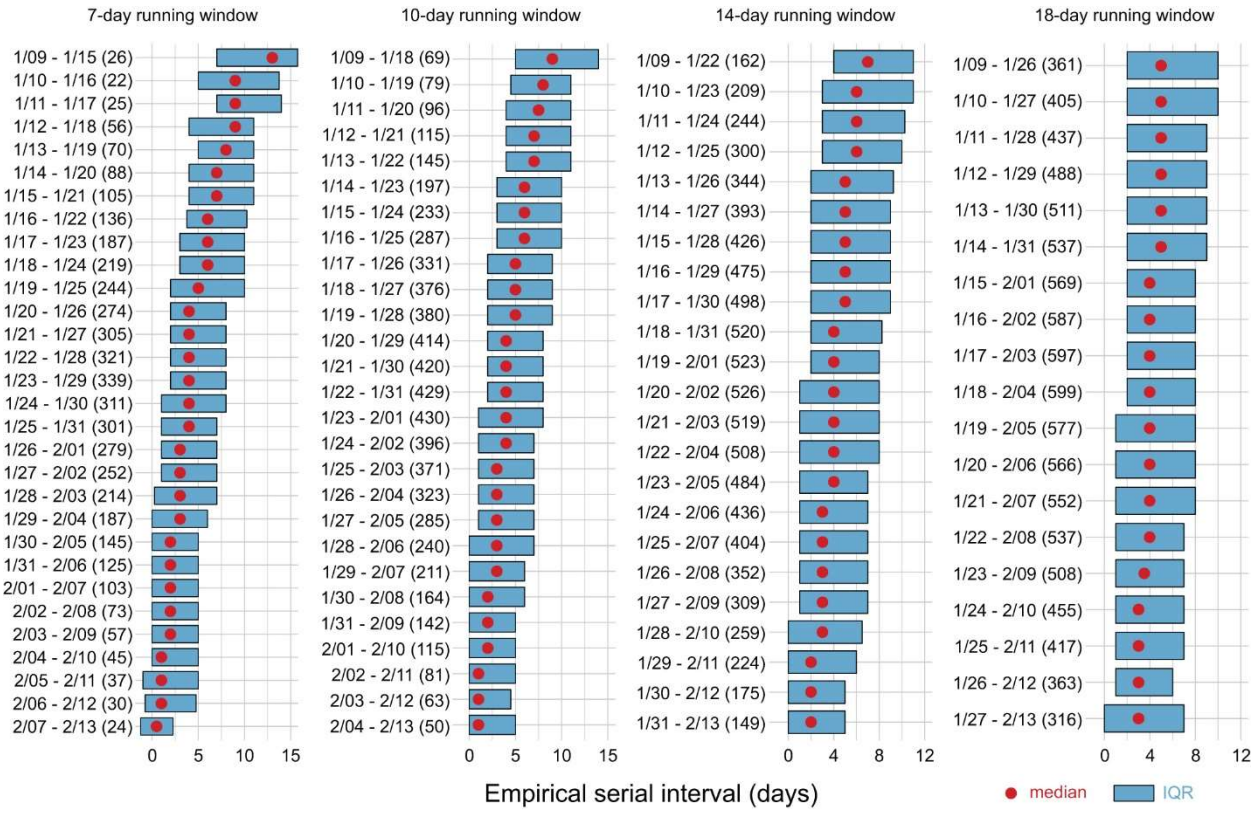

Fig. S10: Empirical distributions of serial interval data in each running time window shifting from January 9 to February 13, 2020. From left to right, each column corresponds to the use of (A) 7-day, (B) 10-day, (C) 14-day, and (D) 18-day running windows, respectively. In each row of each column, the dates and the number on the left-hand side indicate the specific duration and sample size *n* of that time window, and the red dot and blue bar indicate the median and interquartile range (IQR) of serial interval data in that time window, respectively.

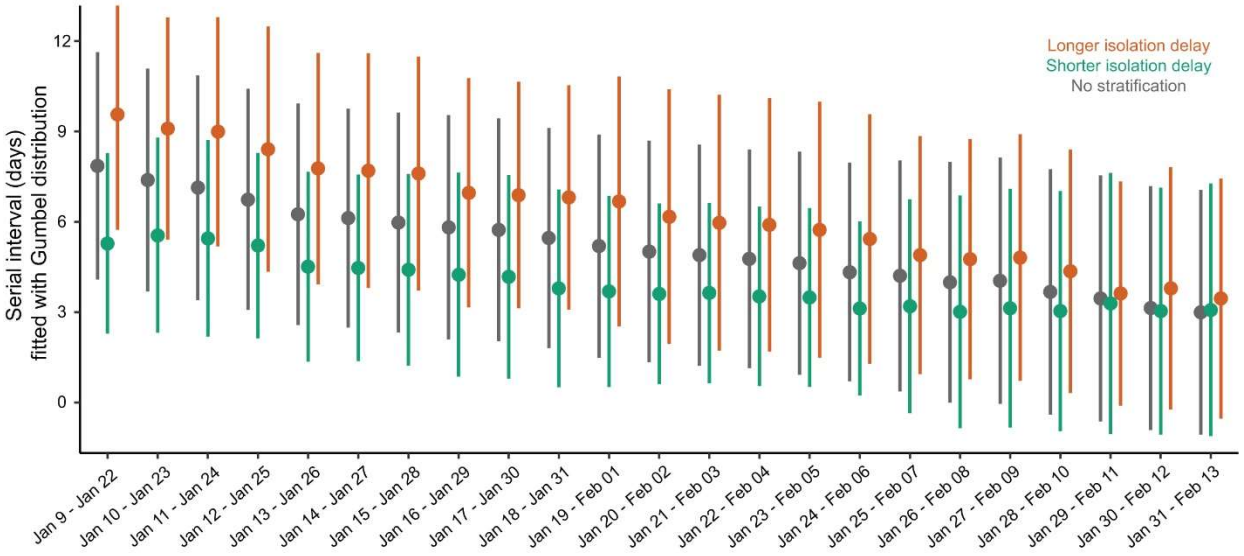

Fig. S11: Serial interval distribution estimated for each of the 14-day running time windows. The first running time window contains the transmission pairs with symptom onset of infectors during January 9 – 22, 2020; the second window contains the transmission pairs with symptom onset of infectors during January 10 – 23, 2020; and so on. Posterior samplers were obtained by fitting a Gumbel distribution to the serial interval data in each time window via MCMC. Dots and bars indicate the median and interquartile range (IQR) for the estimated distribution, respectively. Dark-grey color indicates the fitting for serial interval data with no stratification. Green (orange) indicates the fitting for the data with isolation delay shorter (longer) than the median isolation delay of each running time window.

7.2. Examining the uncertainty in recall bias

The centralized response in mainland China was established by the command system by which the State Council can coordinate a multi-sectoral joint response to promptly mobilize and deploy necessary resources (*48, 49*). Despite this, recall bias may be encountered when suspected or confirmed cases were checking for infection history and epidemiological timelines (e.g. symptom onset dates). As such, we performed a sensitivity analysis to account for the uncertainty in recalling symptom onset date for each case. For example, given a case who developed symptom on day T and a recall bias of τ days, we randomly sampled the onset date of this case between $T - \tau$ and $T + \tau$. We tested the effect of recall bias by using τ =1, 2, or 4 days. This sensitivity analysis validates the robustness of our results (Figs. S12, S13).

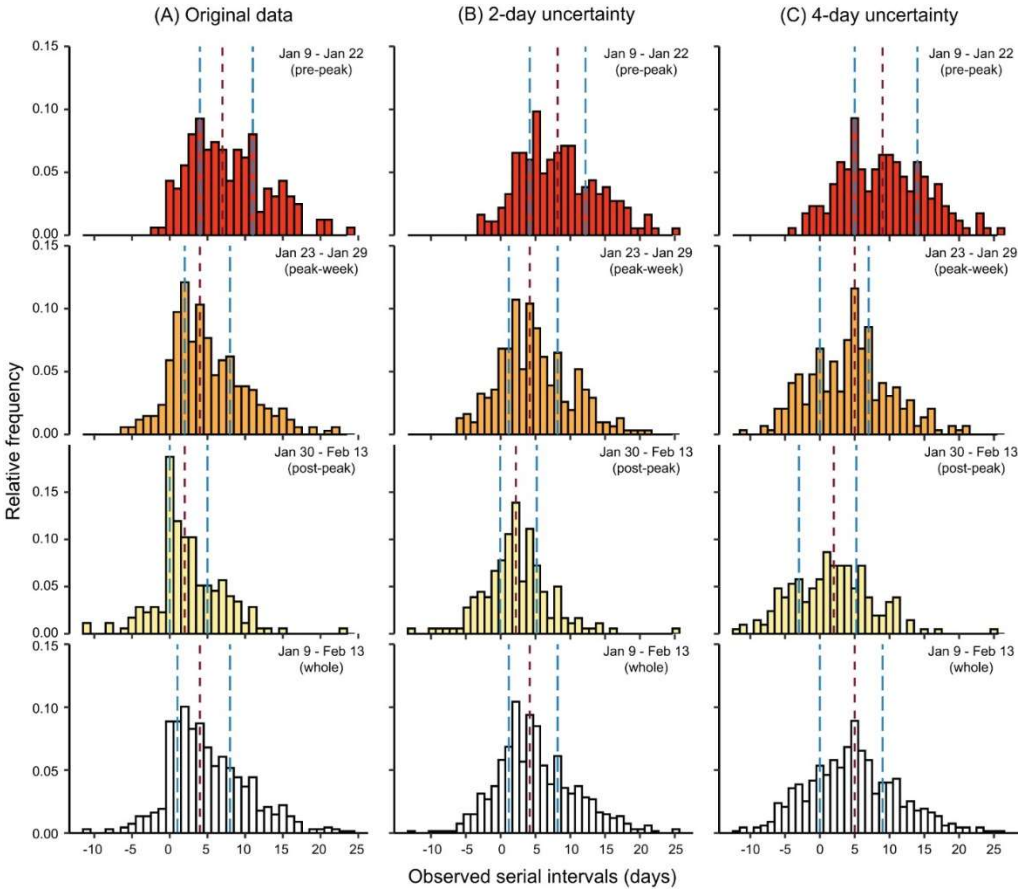

Fig. S12: Sensitivity analysis of empirical serial interval distributions by accounting for uncertainty in recall bias. Left column (A) shows original results without resampling of recall bias. Middle and right columns show the results obtained by resampling the onset date of each case with a recall bias of $\tau = 2$ days (B) and $\tau = 4$ days (C), respectively. In each column, from top to bottom, the transmission pairs were analyzed by selecting infectors who developed symptom during January 9 − 22, 2020 (pre-peak), January 23 − 29, 2020 (peak-week), January 30 − February 13, 2020 (post-peak), and January 9 − February 13, 2020 (whole period), respectively. In each panel, vertical dashed lines in red and blue colors indicate the median and interquartile range (IQR).

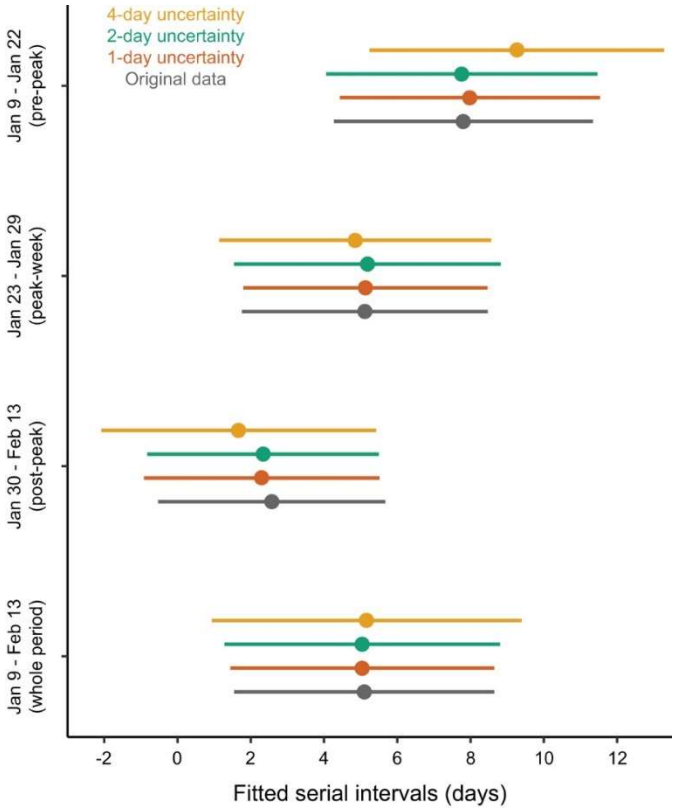

Fig. S13: Sensitivity analysis of the estimated serial interval distributions by accounting for uncertainty in recall bias. Serial interval distribution is estimated by fitting a normal distribution via MCMC. From top to bottom, each group of bars correspond to the transmission pairs with infectors who developed symptom during the pre-peak, peak-week, post-peak, and whole 36-day period, respectively. Dark-grey color shows original results without resampling of recall bias. Other colors show the results obtained by resampling the onset date of each case with a recall bias of τ =1 day (orange), τ =2 days (green), and τ =4 days (yellow), respectively Dots and bars indicate the estimated median and interquartile range (IQR).

7.3. Infector-based serial interval versus transmission pair based serial interval

In our main analysis, the serial interval distributions are calculated in terms of infector-infectee pairs. It is also worth testing the serial interval distribution as the distribution of mean serial interval per infector. If there is significant correlation between the number of infectees and the isolation delay as per infector, then serial interval distribution based on infectors would be

different from that based on transmission pairs. Fig. S14 showsthe distribution of mean serial interval per infector for non-overlapping periods. Compared Fig. S14 to Fig. 1, the infector-based calculation of serial intervals is essentially the same as the transmission pair based calculation of serial intervals.

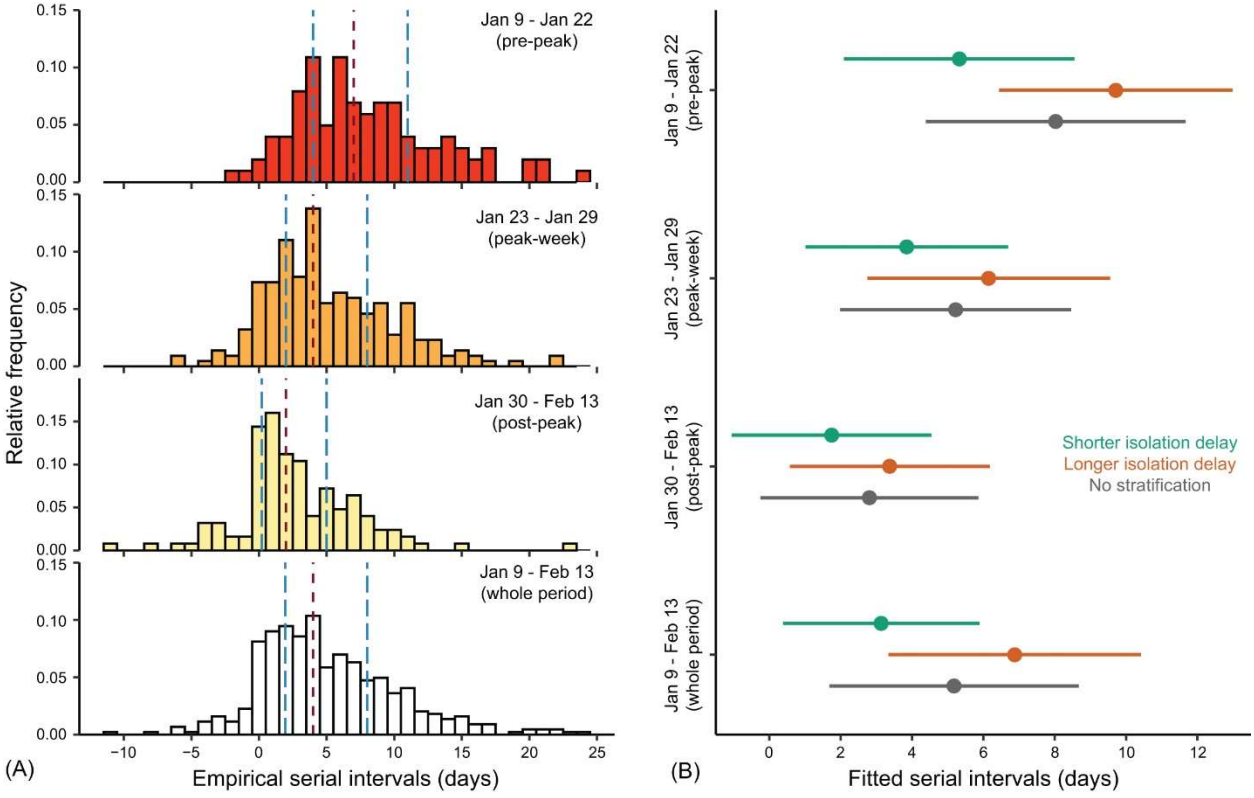

Fig. S14: Temporal change for infector-based serial intervals of COVID-19 in mainland China. (A) Empirical serial interval distributions. From top to bottom, transmission pairs were analyzed by selecting infectors whodeveloped symptom during January 9 − 22, 2020 (pre-peak), January 23 − 29, 2020 (peak-week), January 30 − February 13, 2020 (post-peak), and January 9 − February 13, 2020 (whole period), respectively. In each panel, vertical dashed lines in red and blue colors indicate the median and interquartile range (IQR). (B) Estimated serial interval distributions by fitting a normal distribution via MCMC. From top to bottom, each group of bars correspond to the transmission pairs with infectors who developed symptom during the pre-peak, peak-week, post-peak, and whole 36-day period, respectively. Colored dots and bars correspond to the infectors with isolation delay shorter than the median isolation delay of each period (green), and with isolation delay longer than the median isolation delay of each period (orange), respectively. Dark-grey bars correspond to transmission pairs with no stratification.

Table S1: **Entire dataset of 1,407 transmission pairs in mainland China is available at our GitHub:** https://github.com/PDGLin/COVID19_EffSerialInterval_NPI**(*23*).**

Table S2: Estimated mean and standard deviation (sd) of serial intervals. The columns entitled "Pre-peak period", "Peak-week period", "Post-peak period", and "Whole period" correspond to fitting transmission pair data with infectors developed symptom during the pre-peak period (January 9 − 22, 2020), peak-week period (January 23 − 29, 2020), post-peak period (January 30 − February 13, 2020), and the whole 36-day period (January 9 − February 13, 2020). Each cell in this table presents the estimated median and 95% CrI. Model fitting is performed by fitting a normal distribution via MCMC. Fitting with alternative distributions (e.g., Gumbel distribution) gives similar estimates.

Factors	Pre-peak period			Peak-week period			Post-peak period			Whole period		
	Mean	sd	n	Mean	sd	n	Mean	sd	n	Mean	sd	n
Household	7.2 (5.9, 8.5)	5.4 (4.6, 6.5)	69	5.2 (4.5, 6.0)	5.1 (4.6, 5.7)	175	3.0 (2.0, 3.9)	4.7 (4.1, 5.5)	94	5.0 (4.4, 5.6)	5.2 (4.9, 5.7)	338
Non-household	8.3 (7.2, 9.3)	5.1 (4.5, 6.0)	93	5.0 (4.2, 5.7)	4.9 (4.4, 5.5)	164	2.1 (1.1, 3.1)	4.5 (3.9, 5.3)	82	5.2 (4.6, 5.8)	5.3 (4.9, 5.7)	339
Shorter isolation	5.3 (4.1, 6.4)	4.4 (3.7, 5.4)	60	4.1 (3.3, 4.9)	4.7 (4.2, 5.3)	140	1.6 (0.7, 2.5)	3.9 (3.4, 4.7)	77	3.3 (2.8, 3.8)	4.5 (4.1, 4.9)	292
Longer isolation	9.4 (8.3, 10.4)	5.0 (4.3, 5.8)	91	6.0 (5.2, 6.8)	5.2 (4.7, 5.8)	168	3.4 (2.4, 4.4)	4.6 (4.0, 5.4)	80	6.8 (6.2, 7.3)	5.3 (4.9, 5.7)	324
Younger age	7.4 (6.3, 8.5)	4.9 (4.2, 5.8)	77	5.0 (4.3, 5.8)	4.8 (4.3,5.4)	159	3.2 (2.0, 4.3)	5.1 (4.4, 6.0)	80	5.1 (4.6, 5.7)	5.1 (4.7, 5.5)	316
Older age	8.8 (7.4, 10.0)	5.6 (4.8, 6.6)	74	5.2 (4.5, 6.0)	5.2 (4.7, 5.8)	175	2.1 (1.3, 3.0)	4.2 (3.7, 4.9)	94	5.1 (4.5, 5.7)	5.5 (5.1, 5.9)	343
Male	7.9 (6.9, 9.0)	5.3 (4.6, 6.1)	101	5.1 (4.4, 5.8)	5.3 (4.8, 5.8)	203	2.4 (1.5, 3.2)	4.5 (3.9, 5.1)	114	5.0 (4.5, 5.6)	5.4 (5.1, 5.8)	418
Female	7.8 (6.5, 9.2)	5.2 (4.3, 6.3)	59	5.1 (4.3, 5.9)	4.6 (4.1, 5.2)	133	3.0 (1.7, 4.2)	4.9 (4.1, 5.9)	62	5.2 (4.6, 5.9)	5.0 (4.6, 5.5)	254
All pairs	7.8 (7.0, 8.6)	5.2 (4.7, 5.9)	162	5.1 (4.6, 5.7)	5.0 (4.6, 5.4)	339	2.6 (1.9, 3.2)	4.6 (4.2, 5.1)	176	5.1 (4.7, 5.5)	5.3 (5.0, 5.6)	677

Note: SI=Serial interval, sd= Standard deviation, n=size of the transmission pairs

Table S3: Estimated mean serial intervals for transmission pairs with infectors developed symptom during the early period (first 14-day running time window during January 9 – 22, 2020) and the end period (last 14-day running time window during January 31 – February 13, 2020). Transmission pairs are stratified by different factors (i.e., isolation delay, age, or gender) and settings (i.e., household, non-household, or all transmission pairs). Each cell in this table presents the estimated median and 95% CrI. Model fitting is performed by fitting a normal distribution to the serial interval data truncated by a 14-day time window. Fitting with alternative distributions (e.g., Gumbel distribution) gives similar estimates.

Factors		Household		Non-household		All pairs	
		Early period	End period	Early period	End period	Early period	End period
Isolation delay	Shorter isolation	4.9 (3.1, 6.7)	1.9 (0.5, 3.5)	6.1 (4.5, 7.8)	0.7 (0.0, 2.0)	5.3 (4.1, 6.4)	1.4 (0.5, 2.3)
	Longer isolation	8.9 (7.1, 10.6)	3.1 (1.7, 4.5)	9.6 (8.2, 11.0)	2.6 (1.0, 4.1)	9.4 (8.3, 10.4)	3.0 (1.9, 4.1)
Age	Younger age	6.6 (5.2, 8.1)	3.1 (1.2, 5.0)	8.0 (6.3, 9.6)	2.7 (1.2, 4.3)	7.4 (6.4, 8.6)	2.9 (1.7, 4.1)
	Older age	8.2 (5.8, 10.4)	2.2 (1.0, 3.3)	9.2 (7.7, 10.7)	1.0 (0.1, 2.4)	8.7 (7.5, 10.0)	1.6 (0.7, 2.5)
Gender	Male	7.1 (5.4, 8.8)	1.7 (0.5, 2.9)	8.5 (7.2, 9.8)	2.1 (0.7, 3.5)	7.9 (6.9, 9.0)	1.9 (0.9, 2.8)
	Female	7.6 (5.4, 9.7)	4.7 (2.5, 6.9)	8.1 (6.3, 9.9)	1.5 (0.2, 3.0)	7.8 (6.5, 9.2)	2.8 (1.5, 4.1)
All above factors		7.2 (5.9, 8.5)	2.6 (1.5, 3.6)	8.3 (7.2, 9.3)	1.8 (0.7, 2.8)	7.8 (7.0, 8.6)	2.2 (1.5, 2.9)

Table S4: Estimated mean serial intervals (with the 95% CI in brackets) from the simulated scenarios under different combinations of isolation delay and initial effective reproduction number R_e. We approximated the generation time by serial interval distribution with a mean of 2.6 days in scenario-I, 5.1 days in scenario-II, 7.8 days in scenario-III and 8.4 days in scenario-IV.

Simulated serial intervals (Scenario-I: generation time approximated by serial intervals with mean 2.6 days)							
Isolation delay (d)	**R_e=3.0**	**R_e=2.5**	**R_e=2.0**	**R_e=1.5**	**R_e=1.0**	**R_e=0.5**	**R_e=0.3**
0	1.6 (0.7, 2.3)	1.5 (0.8, 2.2)	1.6 (0.9, 2.2)	1.6 (1.0, 2.0)	1.5 (0.9, 2.1)	1.6 (1.1, 2.1)	1.5 (1.0, 2.0)
1	2.3 (1.5, 2.9)	2.3 (1.5, 2.9)	2.2 (1.5, 2.9)	2.2 (1.5, 2.8)	2.2 (1.7, 2.8)	2.3 (1.7, 2.8)	2.3 (1.7, 2.8)
2	2.6 (1.9, 3.2)	2.5 (1.8, 3.3)	2.6 (1.9, 3.2)	2.6 (1.9, 3.2)	2.6 (2.1, 3.2)	2.6 (2.1, 3.2)	2.6 (2.1, 3.1)
3	2.6 (1.9, 3.3)	2.6 (1.8, 3.3)	2.6 (2.0, 3.3)	2.6 (2.0, 3.2)	2.6 (2.1, 3.2)	2.6 (2.1, 3.1)	2.6 (2.2, 3.1)
4	2.6 (1.8, 3.3)	2.6 (1.8, 3.3)	2.6 (1.8, 3.3)	2.6 (2.0, 3.2)	2.6 (2.0, 3.2)	2.6 (2.1, 3.1)	2.6 (2.1, 3.0)
5	2.6 (1.9, 3.2)	2.6 (1.9, 3.2)	2.6 (2.0, 3.3)	2.6 (1.9, 3.2)	2.6 (2.0, 3.2)	2.6 (2.1, 3.2)	2.6 (2.1, 3.1)
6	2.6 (1.9, 3.3)	2.6 (1.9, 3.3)	2.6 (1.9, 3.1)	2.6 (2.0, 3.2)	2.6 (2.0, 3.2)	2.6 (2.1, 3.2)	2.6 (2.1, 3.1)
7	2.6 (2.0, 3.2)	2.6 (1.8, 3.3)	2.6 (1.8, 3.2)	2.6 (2.0, 3.2)	2.6 (2.1, 3.3)	2.6 (2.1, 3.1)	2.6 (2.1, 3.1)
8	2.6 (1.9, 3.3)	2.6 (1.8, 3.3)	2.6 (1.9, 3.3)	2.6 (2.0, 3.2)	2.6 (2.0, 3.2)	2.6 (2.1, 3.1)	2.6 (2.2, 3.2)
9	2.6 (1.9, 3.4)	2.6 (1.9, 3.3)	2.6 (2.0, 3.3)	2.6 (1.9, 3.2)	2.6 (2.0, 3.1)	2.6 (2.1, 3.2)	2.6 (2.0, 3.1)
10	2.6 (1.8, 3.2)	2.6 (1.9, 3.3)	2.6 (1.9, 3.2)	2.6 (2.0, 3.3)	2.6 (2.0, 3.1)	2.6 (1.9, 3.1)	2.6 (2.1, 3.1)
Simulated serial intervals (Scenario-II: generation time approximated by serial intervals with mean 5.1 days)							
Isolation delay (d)	**R_e=3.0**	**R_e=2.5**	**R_e=2.0**	**R_e=1.5**	**R_e=1.0**	**R_e=0.5**	**R_e=0.3**
0	1.5 (0.8, 2.2)	1.5 (0.8, 2.2)	1.5 (0.7, 2.1)	1.5 (0.9, 2.1)	1.5 (1.0, 2.0)	1.5 (0.9, 1.9)	1.5 (1.0, 2.0)
1	2.3 (1.5, 3.0)	2.3 (1.7, 3.0)	2.3 (1.7, 3.0)	2.3 (1.6, 2.9)	2.3 (1.8, 2.8)	2.4 (1.9, 2.9)	2.3 (1.9, 2.7)
2	3.0 (2.4, 3.7)	3.0 (2.4, 3.5)	3.0 (2.3, 3.8)	3.0 (2.4, 3.6)	3.0 (2.5, 3.6)	3.1 (2.5, 3.6)	3.0 (2.5, 3.6)
3	3.5 (2.8, 4.3)	3.6 (2.8, 4.1)	3.5 (2.8, 4.1)	3.5 (2.9, 4.2)	3.6 (3.0, 4.1)	3.6 (3.0, 4.3)	3.5 (3.1, 4.0)
4	3.9 (3.2, 4.6)	4.0 (3.3, 4.6)	4.0 (3.2, 4.5)	4.0 (3.4, 4.6)	4.0 (3.4, 4.5)	4.0 (3.5, 4.5)	4.0 (3.5, 4.5)
5	4.3 (3.5, 5.0)	4.3 (3.5, 5.0)	4.3 (3.6, 4.8)	4.3 (3.7, 4.9)	4.4 (3.9, 4.9)	4.3 (3.7, 4.9)	4.3 (3.8, 4.9)
6	4.6 (3.8, 5.3)	4.5 (3.9, 5.2)	4.6 (3.8, 5.2)	4.5 (3.8, 5.2)	4.5 (3.9, 5.1)	4.5 (4.0, 5.0)	4.6 (4.0, 5.1)
7	4.7 (3.9, 5.5)	4.7 (4.0, 5.3)	4.7 (4.1, 5.3)	4.7 (4.2, 5.3)	4.7 (4.1, 5.2)	4.7 (4.2, 5.2)	4.7 (4.1, 5.2)
8	4.9 (4.1, 5.5)	4.9 (4.2, 5.5)	4.9 (4.1, 5.6)	4.8 (4.1, 5.5)	4.8 (4.2, 5.3)	4.9 (4.3, 5.4)	4.9 (4.3, 5.4)
9	4.9 (4.1, 5.6)	4.9 (4.2, 5.6)	4.9 (4.3, 5.6)	5.0 (4.2, 5.6)	4.9 (4.3, 5.6)	5.0 (4.4, 5.6)	4.9 (4.4, 5.5)
10	5.1 (4.2, 5.8)	5.0 (4.2, 5.8)	5.0 (4.3, 5.6)	5.0 (4.3, 5.6)	5.0 (4.4, 5.7)	5.0 (4.4, 5.6)	5.0 (4.5, 5.5)
Simulated serial intervals (Scenario-III: generation time approximated by serial intervals with mean 7.8 days)							
Isolation delay (d)	**R_e=3.0**	**R_e=2.5**	**R_e=2.0**	**R_e=1.5**	**R_e=1.0**	**R_e=0.5**	**R_e=0.3**
0	1.2 (0.3, 2.0)	1.3 (0.5, 2.1)	1.3 (0.5, 2.0)	1.3 (0.7, 2.1)	1.3 (0.7, 1.9)	1.3 (0.8, 1.9)	1.3 (0.6, 2.0)
1	2.4 (1.6, 3.1)	2.4 (1.7, 3.0)	2.4 (1.8, 3.1)	2.4 (1.9, 3.0)	2.5 (1.9, 3.1)	2.4 (1.9, 2.9)	2.4 (1.9, 3.1)
2	3.6 (2.8, 4.2)	3.5 (2.8, 4.3)	3.5 (2.8, 4.2)	3.5 (2.9, 4.1)	3.5 (2.8, 4.2)	3.6 (2.9, 4.1)	3.5 (2.9, 4.1)
3	4.6 (3.8, 5.4)	4.6 (3.9, 5.3)	4.6 (3.9, 5.2)	4.6 (4.0, 5.2)	4.6 (4.1, 5.2)	4.6 (4.1, 5.2)	4.6 (4.1, 5.1)
4	5.6 (4.9, 6.3)	5.6 (4.9, 6.4)	5.6 (5.0, 6.3)	5.6 (4.9, 6.2)	5.6 (5.0, 6.1)	5.7 (5.1, 6.1)	5.6 (5.1, 6.1)
5	6.5 (5.8, 7.3)	6.6 (5.8, 7.2)	6.6 (5.9, 7.2)	6.6 (5.9, 7.2)	6.5 (6.0, 7.0)	6.6 (5.9, 7.1)	6.6 (6.1, 7.1)
6	7.3 (6.6, 8.1)	7.3 (6.6, 7.9)	7.3 (6.6, 7.9)	7.3 (6.8, 7.9)	7.3 (6.8, 7.9)	7.3 (6.8, 7.9)	7.3 (6.8, 7.8)
7	7.7 (6.8, 8.4)	7.8 (7.0, 8.5)	7.7 (7.1, 8.4)	7.7 (7.1, 8.2)	7.7 (7.1, 8.4)	7.7 (7.1, 8.2)	7.7 (7.1, 8.2)
8	7.8 (7.0, 8.5)	7.8 (7.0, 8.6)	7.8 (7.1, 8.5)	7.8 (7.2, 8.4)	7.8 (7.2, 8.3)	7.8 (7.3, 8.3)	7.8 (7.3, 8.3)
9	7.8 (6.9, 8.5)	7.8 (7.1, 8.5)	7.8 (7.1, 8.4)	7.8 (7.2, 8.4)	7.8 (7.2, 8.3)	7.8 (7.2, 8.4)	7.8 (7.3, 8.3)
10	7.8 (7.1, 8.5)	7.8 (7.1, 8.4)	7.8 (7.0, 8.5)	7.8 (7.2, 8.3)	7.8 (7.1, 8.4)	7.8 (7.3, 8.3)	7.8 (7.3, 8.4)
Simulated serial intervals (Scenario-IV: generation time approximated by serial intervals with mean 8.4 days)							

Isolation delay (d)	R_e=3.0	R_e=2.5	R_e=2.0	R_e=1.5	R_e=1.0	R_e=0.5	R_e=0.3
0	1.2 (0.4, 2.1)	1.2 (0.4, 2.0)	1.3 (0.4, 2.0)	1.2 (0.5, 1.7)	1.3 (0.6, 1.9)	1.2 (0.6, 1.9)	1.2 (0.5, 2.0)
1	2.4 (1.5, 3.1)	2.3 (1.7, 3.0)	2.3 (1.6, 3.0)	2.4 (1.6, 3.0)	2.4 (1.9, 3.0)	2.3 (1.7, 2.9)	2.4 (1.7, 3.1)
2	3.4 (2.7, 4.3)	3.5 (2.7, 4.2)	3.5 (2.8, 4.2)	3.5 (2.8, 4.2)	3.5 (2.9, 4.0)	3.5 (2.9, 3.9)	3.4 (2.9, 4.0)
3	4.6 (3.8, 5.3)	4.5 (3.8, 5.2)	4.6 (4.0, 5.2)	4.6 (4.0, 5.1)	4.6 (4.1, 5.1)	4.5 (4.1, 5.0)	4.5 (4.0, 5.0)
4	5.6 (4.8, 6.3)	5.7 (5.0, 6.3)	5.7 (5.0, 6.4)	5.6 (5.0, 6.2)	5.6 (5.0, 6.1)	5.6 (5.0, 6.2)	5.6 (5.1, 6.1)
5	6.6 (5.9, 7.5)	6.6 (5.8, 7.4)	6.6 (5.9, 7.2)	6.6 (6.1, 7.3)	6.6 (6.1, 7.2)	6.6 (6.0, 7.1)	6.6 (6.1, 7.1)
6	7.5 (6.8, 8.2)	7.5 (6.8, 8.1)	7.5 (6.8, 8.1)	7.5 (7.0, 8.1)	7.5 (6.9, 8.1)	7.5 (7.0, 8.0)	7.5 (7.1, 8.1)
7	8.2 (7.5, 8.9)	8.1 (7.4, 8.7)	8.2 (7.4, 8.9)	8.1 (7.5, 8.7)	8.1 (7.5, 8.7)	8.2 (7.6, 8.6)	8.1 (7.6, 8.7)
8	8.4 (7.5, 9.2)	8.4 (7.7, 9.0)	8.4 (7.7, 9.1)	8.4 (7.9, 8.9)	8.4 (7.8, 9.0)	8.4 (7.8, 9.0)	8.4 (7.8, 8.9)
9	8.4 (7.6, 9.1)	8.4 (7.8, 9.1)	8.4 (7.6, 9.0)	8.4 (7.8, 9.0)	8.4 (7.9, 9.0)	8.4 (7.9, 8.9)	8.4 (7.8, 9.0)
10	8.4 (7.6, 9.1)	8.4 (7.6, 9.1)	8.4 (7.8, 9.0)	8.4 (7.7, 8.9)	8.4 (7.8, 9.1)	8.4 (7.8, 8.9)	8.4 (7.8, 8.9)

Table S5: Proportions of variance in empirical serial intervals explained by the potential factors from the multi-variable regression models.

Models (Factors)	Household transmissions			Non-household transmissions			All transmissions		
	R^2	$\%\Delta R^2$	df	R^2	$\%\Delta R^2$	df	R^2	$\%\Delta R^2$	df
Isolation delay†	0.3859		23$	0.4685		23$	0.5151	-	34$
+ Isolation of suspected*	0.4255	3.96	22	0.7663	29.78	22$	0.6716	15.64	33
+ Isolation of confirmed*	0.4269	4.10	22	0.7643	29.59	22$	0.6711	15.60	33
+ Inter-city travel ban*	0.3987	1.28	22	0.7317	26.32	22$	0.6473	13.22	33$
+ Intra-city travel ban*	0.4045	1.86	22	0.7278	25.93	22$	0.6557	14.06	33$
+ Closure of public services*	0.4267	4.08	22	0.7734	30.50	22$	0.6823	16.72	33
+ Closure of entertainment venues*	0.4257	3.98	22	0.7685	30.00	22$	0.6765	16.14	33
+ Social mobilization*	0.4135	2.76	22	0.7547	28.62	22$	0.6724	15.73	33

† Basic Model: Predicting empirical serial intervals by accounting for isolation delay only.
* Models improved by combining the basic model with each factor.
$ Statistically significant (both the coefficients for isolation delay and additional factors)
$\%\ \Delta R^2$ measures the change in the explained variance from the model in comparison to the basic model.
i.e. $\%\ \Delta R^2 = (R^2_{models} - R^2_{basic\ model}) \times 100$

References and Notes

1. World Health Organization (WHO), "Coronavirus disease 2019 (COVID-19): Situation report – 162" (WHO, 2020); www.who.int/docs/default-source/coronaviruse/situation-reports/20200629-covid-19-sitrep-161.pdf?sfvrsn=74fde64e_2.

2. M. U. G. Kraemer, C.-H. Yang, B. Gutierrez, C.-H. Wu, B. Klein, D. M. Pigott, Open COVID-19 Data Working Group, L. du Plessis, N. R. Faria, R. Li, W. P. Hanage, J. S. Brownstein, M. Layan, A. Vespignani, H. Tian, C. Dye, O. G. Pybus, S. V. Scarpino, The effect of human mobility and control measures on the COVID-19 epidemic in China. *Science* **368**, 493–497 (2020). doi:10.1126/science.abb4218 Medline

3. C. Wenham, J. Smith, R. Morgan, Gender and COVID-19 Working Group, COVID-19: The gendered impacts of the outbreak. *Lancet* **395**, 846–848 (2020). doi:10.1016/S0140-6736(20)30526-2 Medline

4. J. M. Jin, P. Bai, W. He, F. Wu, X.-F. Liu, D.-M. Han, S. Liu, J.-K. Yang, Gender Differences in Patients With COVID-19: Focus on Severity and Mortality. *Front. Public Health* **8**, 152 (2020). doi:10.3389/fpubh.2020.00152 Medline

5. J. Hellewell, S. Abbott, A. Gimma, N. I. Bosse, C. I. Jarvis, T. W. Russell, J. D. Munday, A. J. Kucharski, W. J. Edmunds, Centre for the Mathematical Modelling of Infectious Diseases COVID-19 Working Group, S. Funk, R. M. Eggo, Feasibility of controlling COVID-19 outbreaks by isolation of cases and contacts. *Lancet Glob. Health* **8**, e488–e496 (2020). doi:10.1016/S2214-109X(20)30074-7 Medline

6. L. Ferretti, C. Wymant, M. Kendall, L. Zhao, A. Nurtay, L. Abeler-Dörner, M. Parker, D. Bonsall, C. Fraser, Quantifying SARS-CoV-2 transmission suggests epidemic control with digital contact tracing. *Science* **368**, eabb6936 (2020). doi:10.1126/science.abb6936 Medline

7. R. Armitage, L. B. Nellums, COVID-19 and the consequences of isolating the elderly. *Lancet Public Health* **5**, e256 (2020). doi:10.1016/S2468-2667(20)30061-X Medline

8. R. M. Anderson, H. Heesterbeek, D. Klinkenberg, T. D. Hollingsworth, How will country-based mitigation measures influence the course of the COVID-19 epidemic? *Lancet* **395**, 931–934 (2020). doi:10.1016/S0140-6736(20)30567-5 Medline

9. J. R. Koo, A. R. Cook, M. Park, Y. Sun, H. Sun, J. T. Lim, C. Tam, B. L. Dickens, Interventions to mitigate early spread of SARS-CoV-2 in Singapore: A modelling study. *Lancet Infect. Dis.* **20**, 678–688 (2020). doi:10.1016/S1473-3099(20)30162-6 Medline

10. K. Prem, Y. Liu, T. W. Russell, A. J. Kucharski, R. M. Eggo, N. Davies, Centre for the Mathematical Modelling of Infectious Diseases COVID-19 Working Group, M. Jit, P. Klepac, The effect of control strategies to reduce social mixing on outcomes of the COVID-19 epidemic in Wuhan, China: A modelling study. *Lancet Public Health* **5**, e261–e270 (2020). doi:10.1016/S2468-2667(20)30073-6 Medline

11. M. A. Vink, M. C. Bootsma, J. Wallinga, Serial intervals of respiratory infectious diseases: A systematic review and analysis. *Am. J. Epidemiol.* **180**, 865–875 (2014). doi:10.1093/aje/kwu209 Medline

12. J. T. Wu, K. Leung, G. M. Leung, Nowcasting and forecasting the potential domestic and international spread of the 2019-nCoV outbreak originating in Wuhan, China: A modelling study. *Lancet* **395**, 689–697 (2020). doi:10.1016/S0140-6736(20)30260-9 Medline

13. M. Chinazzi, J. T. Davis, M. Ajelli, C. Gioannini, M. Litvinova, S. Merler, A. Pastore Y Piontti, K. Mu, L. Rossi, K. Sun, C. Viboud, X. Xiong, H. Yu, M. E. Halloran, I. M. Longini Jr., A. Vespignani, The effect of travel restrictions on the spread of the 2019 novel coronavirus (COVID-19) outbreak. *Science* **368**, 395–400 (2020). doi:10.1126/science.aba9757 Medline

14. H. Nishiura, N. M. Linton, A. R. Akhmetzhanov, Serial interval of novel coronavirus (COVID-19) infections. *Int. J. Infect. Dis.* **93**, 284–286 (2020). doi:10.1016/j.ijid.2020.02.060 Medline

15. H. Y. Cheng, S.-W. Jian, D.-P. Liu, T.-C. Ng, W.-T. Huang, H.-H. Lin, Taiwan COVID-19 Outbreak Investigation Team, Contact Tracing Assessment of COVID-19 Transmission Dynamics in Taiwan and Risk at Different Exposure Periods Before and After Symptom Onset. *JAMA Intern. Med.* 10.1001/jamainternmed.2020.2020 (2020). doi:10.1001/jamainternmed.2020.2020 Medline

16. Z. Du, X. Xu, Y. Wu, L. Wang, B. J. Cowling, L. A. Meyers, Serial Interval of COVID-19 among Publicly Reported Confirmed Cases. *Emerg. Infect. Dis.* **26**, 1341–1343 (2020). doi:10.3201/eid2606.200357 Medline

17. Q. Li, X. Guan, P. Wu, X. Wang, L. Zhou, Y. Tong, R. Ren, K. S. M. Leung, E. H. Y. Lau, J. Y. Wong, X. Xing, N. Xiang, Y. Wu, C. Li, Q. Chen, D. Li, T. Liu, J. Zhao, M. Liu, W. Tu, C. Chen, L. Jin, R. Yang, Q. Wang, S. Zhou, R. Wang, H. Liu, Y. Luo, Y. Liu, G. Shao, H. Li, Z. Tao, Y. Yang, Z. Deng, B. Liu, Z. Ma, Y. Zhang, G. Shi, T. T. Y. Lam, J. T. Wu, G. F. Gao, B. J. Cowling, B. Yang, G. M. Leung, Z. Feng, Early Transmission Dynamics in Wuhan, China, of Novel Coronavirus-Infected Pneumonia. *N. Engl. J. Med.* **382**, 1199–1207 (2020). doi:10.1056/NEJMoa2001316 Medline

18. J. M. Griffin, A. B. Collins, K. Hunt, D. McEvoy, M. Casey, A. W. Byrne, C. G. McAloon, A. Barber, E. A. Lane, S. J. More, A rapid review of available evidence on the serial interval and generation time of COVID-19. medRxiv 2020.05.08.20095075 [Preprint]. 11 May 2020. https://doi.org/10.1101/2020.05.08.20095075.

19. S. Ma, J. Zhang, M. Zeng, Q. Yun, W. Guo, Y. Zheng, S. Zhao, M. H. Wang, Z. Yang, Epidemiological parameters of coronavirus disease 2019: A pooled analysis of publicly reported individual data of 1155 cases from seven countries. medRxiv 2020.03.21.20040329 [Preprint]. 24 March 2020. https://doi.org/10.1101/2020.03.21.20040329.

20. X. He, E. H. Y. Lau, P. Wu, X. Deng, J. Wang, X. Hao, Y. C. Lau, J. Y. Wong, Y. Guan, X. Tan, X. Mo, Y. Chen, B. Liao, W. Chen, F. Hu, Q. Zhang, M. Zhong, Y. Wu, L. Zhao, F. Zhang, B. J. Cowling, F. Li, G. M. Leung, Temporal dynamics in viral shedding and transmissibility of COVID-19. *Nat. Med.* **26**, 672–675 (2020). doi:10.1038/s41591-020-0869-5 Medline

21. Q. Bi, Y. Wu, S. Mei, C. Ye, X. Zou, Z. Zhang, X. Liu, L. Wei, S. A. Truelove, T. Zhang, W. Gao, C. Cheng, X. Tang, X. Wu, Y. Wu, B. Sun, S. Huang, Y. Sun, J. Zhang, T. Ma, J.

Lessler, T. Feng, Epidemiology and transmission of COVID-19 in 391 cases and 1286 of their close contacts in Shenzhen, China: A retrospective cohort study. *Lancet Infect. Dis.* **20**, 911–919 (2020). doi:10.1016/S1473-3099(20)30287-5 Medline

22. J. Zhang, M. Litvinova, Y. Liang, Y. Wang, W. Wang, S. Zhao, Q. Wu, S. Merler, C. Viboud, A. Vespignani, M. Ajelli, H. Yu, Changes in contact patterns shape the dynamics of the COVID-19 outbreak in China. *Science* **368**, 1481–1486 (2020). doi:10.1126/science.abb8001 Medline

23. Lin, PDGLin/COVID19_EffSerialInterval_NPI: Serial interval of SARS-CoV-2 was shortened over time by non-pharmaceutical interventions, version v1.0, Zenodo (2020); http://doi.org/10.5281/zenodo.3940300.

24. H. Tian, Y. Liu, Y. Li, C.-H. Wu, B. Chen, M. U. G. Kraemer, B. Li, J. Cai, B. Xu, Q. Yang, B. Wang, P. Yang, Y. Cui, Y. Song, P. Zheng, Q. Wang, O. N. Bjornstad, R. Yang, B. T. Grenfell, O. G. Pybus, C. Dye, An investigation of transmission control measures during the first 50 days of the COVID-19 epidemic in China. *Science* **368**, 638–642 (2020). doi:10.1126/science.abb6105 Medline

25. K. Leung, J. T. Wu, D. Liu, G. M. Leung, First-wave COVID-19 transmissibility and severity in China outside Hubei after control measures, and second-wave scenario planning: A modelling impact assessment. *Lancet* **395**, 1382–1393 (2020). doi:10.1016/S0140-6736(20)30746-7 Medline

26. A. Pan, L. Liu, C. Wang, H. Guo, X. Hao, Q. Wang, J. Huang, N. He, H. Yu, X. Lin, S. Wei, T. Wu, Association of Public Health Interventions With the Epidemiology of the COVID-19 Outbreak in Wuhan, China. *JAMA* **323**, 1915–1923 (2020). doi:10.1001/jama.2020.6130 Medline

27. J. Zhang, M. Litvinova, W. Wang, Y. Wang, X. Deng, X. Chen, M. Li, W. Zheng, L. Yi, X. Chen, Q. Wu, Y. Liang, X. Wang, J. Yang, K. Sun, I. M. Longini Jr., M. E. Halloran, P. Wu, B. J. Cowling, S. Merler, C. Viboud, A. Vespignani, M. Ajelli, H. Yu, Evolving epidemiology and transmission dynamics of coronavirus disease 2019 outside Hubei province, China: A descriptive and modelling study. *Lancet Infect. Dis.* **20**, 793–802 (2020). doi:10.1016/S1473-3099(20)30230-9 Medline

28. A. Cori, N. M. Ferguson, C. Fraser, S. Cauchemez, A new framework and software to estimate time-varying reproduction numbers during epidemics. *Am. J. Epidemiol.* **178**, 1505–1512 (2013). doi:10.1093/aje/kwt133 Medline

29. L. Zou, F. Ruan, M. Huang, L. Liang, H. Huang, Z. Hong, J. Yu, M. Kang, Y. Song, J. Xia, Q. Guo, T. Song, J. He, H.-L. Yen, M. Peiris, J. Wu, SARS-CoV-2 Viral Load in Upper Respiratory Specimens of Infected Patients. *N. Engl. J. Med.* **382**, 1177–1179 (2020). doi:10.1056/NEJMc2001737 Medline

30. Y. Pan, D. Zhang, P. Yang, L. L. M. Poon, Q. Wang, Viral load of SARS-CoV-2 in clinical samples. *Lancet Infect. Dis.* **20**, 411–412 (2020). doi:10.1016/S1473-3099(20)30113-4 Medline

31. X. K. Xu, X.-F. Liu, Y. Wu, S. T. Ali, Z. Du, P. Bosetti, E. H. Y. Lau, B. J. Cowling, L. Wang, Reconstruction of Transmission Pairs for novel Coronavirus Disease 2019 (COVID-19) in mainland China: Estimation of Super-spreading Events, Serial Interval,

and Hazard of Infection. *Clin. Infect. Dis.* 10.1093/cid/ciaa790 (2020). doi:10.1093/cid/ciaa790 Medline

32. P. Trapman, F. Ball, J.-S. Dhersin, V. C. Tran, J. Wallinga, T. Britton, Inferring R0 in emerging epidemics-the effect of common population structure is small. *J. R. Soc. Interface* **13**, 20160288 (2016). doi:10.1098/rsif.2016.0288 Medline

33. S. W. Park, D. Champredon, J. Dushoff, Inferring generation-interval distributions from contact-tracing data. *J. R. Soc. Interface* **17**, 20190719 (2020). doi:10.1098/rsif.2019.0719 Medline

34. Q. H. Liu, M. Ajelli, A. Aleta, S. Merler, Y. Moreno, A. Vespignani, Measurability of the epidemic reproduction number in data-driven contact networks. *Proc. Natl. Acad. Sci. U.S.A.* **115**, 12680–12685 (2018). doi:10.1073/pnas.1811115115 Medline

35. Y. Bai, L. Yao, T. Wei, F. Tian, D.-Y. Jin, L. Chen, M. Wang, Presumed Asymptomatic Carrier Transmission of COVID-19. *JAMA* **323**, 1406–1407 (2020). doi:10.1001/jama.2020.2565 Medline

36. X. Pan, D. Chen, Y. Xia, X. Wu, T. Li, X. Ou, L. Zhou, J. Liu, Asymptomatic cases in a family cluster with SARS-CoV-2 infection. *Lancet Infect. Dis.* **20**, 410–411 (2020). doi:10.1016/S1473-3099(20)30114-6 Medline

37. M. M. Arons, K. M. Hatfield, S. C. Reddy, A. Kimball, A. James, J. R. Jacobs, J. Taylor, K. Spicer, A. C. Bardossy, L. P. Oakley, S. Tanwar, J. W. Dyal, J. Harney, Z. Chisty, J. M. Bell, M. Methner, P. Paul, C. M. Carlson, H. P. McLaughlin, N. Thornburg, S. Tong, A. Tamin, Y. Tao, A. Uehara, J. Harcourt, S. Clark, C. Brostrom-Smith, L. C. Page, M. Kay, J. Lewis, P. Montgomery, N. D. Stone, T. A. Clark, M. A. Honein, J. S. Duchin, J. A. Jernigan, Public Health–Seattle and King County and CDC COVID-19 Investigation Team, Presymptomatic SARS-CoV-2 Infections and Transmission in a Skilled Nursing Facility. *N. Engl. J. Med.* **382**, 2081–2090 (2020). doi:10.1056/NEJMoa2008457 Medline

38. T. Ganyani, C. Kremer, D. Chen, A. Torneri, C. Faes, J. Wallinga, N. Hens, Estimating the generation interval for coronavirus disease (COVID-19) based on symptom onset data, March 2020. *Euro Surveill.* **25**, 2000257 (2020). doi:10.2807/1560-7917.ES.2020.25.17.2000257 Medline

39. W. E. Wei, Z. Li, C. J. Chiew, S. E. Yong, M. P. Toh, V. J. Lee, Presymptomatic Transmission of SARS-CoV-2 - Singapore, January 23-March 16, 2020. *MMWR Morb. Mortal. Wkly. Rep.* **69**, 411–415 (2020). doi:10.15585/mmwr.mm6914e1 Medline

40. L. Tindale, M. Coombe, J. E. Stockdale, E. Garlock, W. Y. V. Lau, M. Saraswat, Y.-H. B. Lee, L. Zhang, D. Chen, J. Wallinga, C. Colijn, Transmission interval estimates suggest pre-symptomatic spread of COVID-19. medRxiv 2020.03.03.20029983 [Preprint]. 6 March 2020. https://doi.org/10.1101/2020.03.03.20029983.

41. R. Wölfel, V. M. Corman, W. Guggemos, M. Seilmaier, S. Zange, M. A. Müller, D. Niemeyer, T. C. Jones, P. Vollmar, C. Rothe, M. Hoelscher, T. Bleicker, S. Brünink, J. Schneider, R. Ehmann, K. Zwirglmaier, C. Drosten, C. Wendtner, Virological assessment of hospitalized patients with COVID-2019. *Nature* **581**, 465–469 (2020). doi:10.1038/s41586-020-2196-x Medline

42. A. T. Huang, B. Garcia-Carreras, M. D. T. Hitchings, B. Yang, L. Katzelnick, S. M. Rattigan, B. Borgert, C. Moreno, B. D. Solomon, I. Rodriguez-Barraquer, J. Lessler, H. Salje, D. S. Burke, A. Wesolowski, D. A. T. Cummings, A systematic review of antibody mediated immunity to coronaviruses: Antibody kinetics, correlates of protection, and association of antibody responses with severity of disease. medRxiv 2020.04.14.20065771 [Preprint]. 17 April 2020. https://doi.org/10.1101/2020.04.14.20065771.

43. B. Rockx, T. Kuiken, S. Herfst, T. Bestebroer, M. M. Lamers, B. B. Oude Munnink, D. de Meulder, G. van Amerongen, J. van den Brand, N. M. A. Okba, D. Schipper, P. van Run, L. Leijten, R. Sikkema, E. Verschoor, B. Verstrepen, W. Bogers, J. Langermans, C. Drosten, M. Fentener van Vlissingen, R. Fouchier, R. de Swart, M. Koopmans, B. L. Haagmans, Comparative pathogenesis of COVID-19, MERS, and SARS in a nonhuman primate model. *Science* **368**, 1012–1015 (2020). doi:10.1126/science.abb7314 Medline

44. M. Lipsitch, T. Cohen, B. Cooper, J. M. Robins, S. Ma, L. James, G. Gopalakrishna, S. K. Chew, C. C. Tan, M. H. Samore, D. Fisman, M. Murray, Transmission dynamics and control of severe acute respiratory syndrome. *Science* **300**, 1966–1970 (2003). doi:10.1126/science.1086616 Medline

45. K. M. Gostic, L. McGough, E. Baskerville, S. Abbott, K. Joshi, C. Tedijanto, R. Kahn, R. Niehus, J. A. Hay, P. M. De Salazar, J. Hellewell, S. Meakin, J. Munday, N. Bosse, K. Sherratt, R. M. Thompson, L. F. White, J. Huisman, J. Scire, S. Bonhoeffer, T. Stadler, J. Wallinga, S. Funk, M. Lipsitch, S. Cobey, Practical considerations for measuring the effective reproductive number, Rt. medRxiv 2020.06.18.20134858 [Preprint]. 23 June 2020. https://doi.org/10.1101/2020.06.18.20134858.

46. J. Wallinga, P. Teunis, Different epidemic curves for severe acute respiratory syndrome reveal similar impacts of control measures. *Am. J. Epidemiol.* **160**, 509–516 (2004). doi:10.1093/aje/kwh255 Medline

47. C. Fraser, Estimating individual and household reproduction numbers in an emerging epidemic. *PLOS ONE* **2**, e758 (2007). doi:10.1371/journal.pone.0000758 Medline

48. Z. Li, Q. Chen, L. Feng, L. Rodewald, Y. Xia, H. Yu, R. Zhang, Z. An, W. Yin, W. Chen, Y. Qin, Z. Peng, T. Zhang, D. Ni, J. Cui, Q. Wang, X. Yang, M. Zhang, X. Ren, D. Wu, X. Sun, Y. Li, L. Zhou, X. Qi, T. Song, G. F. Gao, Z. Feng, China CDC COVID-19 Emergency Response Strategy Team, Active case finding with case management: The key to tackling the COVID-19 pandemic. *Lancet* **396**, 63–70 (2020). doi:10.1016/S0140-6736(20)31278-2 Medline

49. P. Wu, X. Hao, E. H. Y. Lau, J. Y. Wong, K. S. M. Leung, J. T. Wu, B. J. Cowling, G. M. Leung, Real-time tentative assessment of the epidemiological characteristics of novel coronavirus infections in Wuhan, China, as at 22 January 2020. *Euro Surveill.* **25**, 2000044 (2020). doi:10.2807/1560-7917.ES.2020.25.3.2000044 Medline